sciendo

Polish Journal of Chemical Technology, 22, 1, 35—45, 10.2478/pjct-2020-0006

Optimization the operation parameters of SDA desulfurization tower by flow coupling chemical reaction model

Dan Mei[1, 2], Junjie Shi[1], Yuzheng Zhu[1], Xuemei Xu[1], Futang Xing[1, 2*],Ling Shi[2]

[1]*Hubei Key Laboratory for Efficient Utilization and Agglomeration of Metallurgic Mineral Resources, Wuhan University of Science and Technology, Wuhan 430081, China*
[2]*Hubei Key Laboratory of Industrial Fume & Dust Pollution Control, Jianghan University, Wuhan 430056, China*
[*]*Corresponding authors: e-mail: xing_futang@163.com*

Spray Drying Absorber (SDA) has been widely used for large-scale desulfurization. However, it also has some limitations. For example, the liquid absorbent easily causes scaling, which impedes the contact between the serous fluid and the flue gas and reduces the chemical reaction rate and desulfurization efficiency. This paper establishes the mathematical and physical model of gas and liquid two-phase flow and droplet evaporation and heat transfer in rotary spray desulfurization tower. To study the accumulation and distribution of chemical reaction precipitates in the desulfurization tower and analyze the removal efficiency of sulfur dioxide (SO_2) in different atomization diameters, this paper establishes a simulation model concerning the coupling of desulfurization reaction and flow field calculation based on the absorption and reaction mechanism of SO_2. Baffle in different widths are set to optimize the internal flow field and balance the distribution of flue gas. By setting baffles of different widths to optimize the flow field in the tower and changing the distribution of flue gas, this model reduces the scaling while ensuring the desulfurization efficiency. The results of the simulation experiment have verified that the droplet with a diameter of 50 μm is the optimal option, which can effectively remove the scaling and ensure that the desulfurizing tower runs in high efficiency and stability. When the width of baffles is 2250 mm, the efficiency of desulfurization exceeds 95%, and the amount of scaling on the desulfurization tower main wall is controlled at the minimum level, which is the optimal option for production.

Keywords: spray drying absorber tower; gas-liquid two-phase flow; droplet diameter; desulfurization efficiency; amount of scaling

INTRODUCTION

As one of the major air pollutants, sulfur dioxide (SO_2) poses a great threat to the ecological environment. By contributing to acid rain, it can have significant impacts on humans, animals and plants. For humans, when SO_2 is breathed in, most of them is retained in the upper respiratory tract. Then sulfurous acid with corrosiveness will form on the wet mucous membrane, with part of them being oxidized to sulfuric acid, which will irritate the respiratory system. If a human inhales SO_2 at the concentration of 100 ppm at one time, there will be obvious irritation sign of bronchial and lungs. More seriously, the lung tissues will be damaged in eight hours without timely treat and cure. As SO_2 can be absorbed into the blood, it can poison the other parts of the body by destroying the enzymatic activities, reducing the human metabolism, and damaging the liver function[1].

During the sintering process of steel, a large amount of SO_2 is produced and emitted with the concentration between 400 to 2000 mg/m^3, which may cause huge pollution to the environment. Therefore, to reduce the emission of SO_2, the desulfurizing techniques should be adopted during this process.

Developed by a Denmark company called GEA Niro in the 1970s, Spray drying absorber (SDA) is a large-scale desulfurization method used by companies all over the world. The specific workflows of SDA are showed as follows: A high-speed motor drives the atomizing wheel to rotate at a high speed, generating a strong centrifugal force. Then the turbid liquid or emulsion with alkaline substance $Ca(OH)_2$ is spouted out and atomized into micro-sized droplets through the nozzle on the atomizing wheel and then evenly sprayed into the reaction zone inside the tower[2]. The sintering flue gas enters the tower through the flue gas distributor and then thoroughly contacts with the atomized droplets of $Ca(OH)_2$, of which the acidic substances are neutralized in a short time for desulfurization. Meanwhile, the dry resultants formed in the acid-base neutralization reaction accumulating inside the tower are collected in the bag-type dust collector.

The SDA method possesses many advantages. For example, it can easily adapt to the changes of smoke compositions, flow rate, temperature, and concentration of SO_2, with simple workflows and high efficiency of desulfurization. Moreover, the by-products can be recycled[3]. However, this method also has some limitations. As the absorbent is liquid, scaling can be caused (as shown in Fig. 1), which changes the air flow distribution inside the tower. As a result, the contact between the serous fluid and the flue gas will be impeded, which lowers the chemical reaction rate and desulfurization efficiency[4].

Figure 1. Scaling on the distributor in the desulfurization tower

With the popularization of rotary spray and drying technology, many scholars and researchers have conducted researches on the acid-base absorption reaction, gas-liquid flow and heat-transfer characteristics of the desulfurizing tower, particularly on the solid component content of alkaline particles in the serous fluid, the concentration of SO_2 in the flue gas, the ratio of Ca/S and SO_2 in the serous fluid as well as the drying time of the serous fluid. The numerical simulation method has been adopted to study the factors which can improve the desulfurization efficiency of the flue gas, such as flue gas temperature, atomization and evaporation characteristics of the serous fluid, as well as gas flow structure.

HT Karlsson[5] suggested that the concentration of lime slurry significantly influenced the desulfurization process. By studying the influence of the concentration of serous fluid on the desulfurization efficiency through experiments, he found that if there were too much solid lime particles in the serous fluid, the diffusion of SO_2 on the surface of the serous fluid would be impeded. With SO_2 failing to react with the serous fluid completely, the desulfurization efficiency was thus lowered. But if the lime slurry was in moderate concentration , the concentration of SO_2 in the flue gas had no obvious impact on the desulfurization efficiency.

According to the research of FF. Hill[6], the absorption efficiency of SO_2 was related to the drying condition when the $Ca(OH)_2$ content was relatively high. However, under this circumstance, the mass transfer resistance of liquid would be the main factor to lower the absorption efficiency. Gullett[7] studied the characteristics of the serous fluid particles in the absorbent and the concentration of SO_2 in the desulfurization reaction. The research results indicated that the overall reaction rate was impacted by the diffusion of gas film when the concentration of SO_2 was lower than 800 ppm. However, when the concentration of SO_2 was higher than 800 ppm, the reaction rate was controlled by the dissolution rate of lime. According to the previous studies analyzing the influence of the calcium-sulfur ratio on the desulfurization efficiency through the laboratory reactor[8], it was found that if the calcium-sulfur ratio reached 1.2, the removal rate of SO_2 would exceed 95%.

Studying the reaction process of the serous fluid and flue gas, SR Dantuluri[9], Wentz[10] and Ranz[11] divided the serous fluid evaporation and desulfurization reaction into three stages, which were the normal-speed reaction stage, the slow-down reaction stage, and the quasi-equilibrium reaction stage. Partridge[12] holds that as the serous fluid droplets were heated continuously in the slow-down reaction stage, the surface of the large particles would be dry, with small pores on it. That is, when the serous fluid lost a large amount of water, a shell would be formed on the surface of the solid particle clusters to block the contact between the flue gas and the serous fluid. As a result, the desulfurization reaction would be terminated.

Studying on the spray drying process through experiment, Sang SK[13] found that when the SO_2 molecules were fully exposed to the wet droplets, the total surface area of droplet was the key factor imparting the desulfurization process. If the atomized droplets were too small or the evaporation speed was too fast, the shell forming in a short time on the surface will prevent the SO_2 molecules from sufficiently transferring to the surface of the droplets, which would lower the desulfurization efficiency.

By adding hygroscopic agent to prolong the liquid state of serous fluid, TC Keener[14] improved the utilization of lime and the removal rate of SO_2. He found that over 90% of SO_2 was removed when additives were used moderately.

A theoretical model of the semi-dry flue gas desulfurization method has been built by Chen Minggong[15]. The retention time of the serous fluid in the desulfurization tower was calculated based on the desulfurizing reaction model and the drying model. He found that when the desulfurizing reaction time was longer than the drying time, the factors deciding the retention time of serous fluid ware SO_2 content in the flue gas, the liquid-phase diffusion coefficient of the SO_2 molecules, the reaction rate constant, the concentration of $Ca(OH)_2$ in the absorption liquid, and the mass transfer coefficient of the SO_2 liquid film. However, when the drying time was longer than the desulfurization time, factors that decided the retention time were evaporation amount, the droplet density, the vaporization enthalpy of solution and gas, the heat conductivity coefficient, and the temperature of flue gas and droplets.

As for the studies on the influence of droplet evaporation, H Kim[16] has conducted numerical simulation researches and found that in low temperature, the evaporation time of droplets would become longer with the increase of pressure, while in high temperature, the evaporation time would get shortened with the increase of pressure. A mathematical model concerning the droplet movement and evaporation in the gas flue has been established by Kang Meiqiang[17], to study the impacts of parameters, including flue structure, flue gas temperature, spray particle diameter and installation position of the nozzle, on evaporation characteristics. Moreover, Han Fangliang[18] simulated the three-dimensional flow field inside the flue gas desulfurization tower based on the turbulence model and random orbit model, which optimized the operation conditions of the desulfurization tower.

To research the influence of various operating parameters on desulfurization efficiency, Fabrizio Scala[19–21] established a steady-state one-dimensional spray dryer model and a single-molecule rigid droplet model of SO_2 absorption to conduct the numerical simulation on the instantaneous and irreversible chemical reactions occurs in the desulfurization tower. It was found that the Ca/S molar feed ratio, average initial droplet size and lime particle size had a significant influence on the desulfurization efficiency. Chen Jianzhong[22] suggested that temperature drop and temperature difference of adiabatic saturation of the flue gas in the desulfurization tower had a great impact on the desulfurization efficiency. He held that as the reaction time of liquid desulfurization became longer, the evaporation time of droplets would be affected, causing the desulfurization efficiency drop exponentially with the adiabatic saturation temperature rising. Establishing an integrated model applicable to the semi-dry desulfurization tower and the bag-type dust collector and considering the gas-phase resistance, liquid-phase mass transfer resistance and lime dissolution

resistance, Wang Naihua[23] has conducted researches on calcium-sulfur ratio, adiabatic saturated temperature, the initial particle diameter of limestone serous fluid, and the flue gas temperature at the SO_2 inlet.

The simultaneous removal of SO_2 and polycyclic aromatic hydrocarbons (PAHs) by adding calcium-based additives CaO, $Ca(OH)_2$, and $CaCO_3$ during sewage sludge incineration was investigated in a fluidized bed incinerator by Qin Linbo and Han Jun[24]. Novel integrated desulfurization (NID) technology applied for sintering flue gas SO_2 removal was studied to investigate the effects of approach to saturation temperature, CaO/S and H_2O/CaO on SO_2 removal efficiency by Qin Linbo[25]. Separate gasification of Fenton-oxidized or CaO-treated sludge released H_2S emission respectively from sulfonic acid/sulfone/heterocyclic-S and inorganic sulfide in char was studied by Liu Huan[26]. Qin Linbo[27] studied the effect of sewage sludge-CaO weight ratio, calcination temperature and hydration time on desulfurization efficiency. He found that SO_2 removal efficiency was increased from 88.7% to 97.3% after using the lime modified with sewage sludge.

The SDA technology has been widely investigated from the early time, and great achievements has been gained in theory and experimental research. However, the former researches mainly studied the factors which influence the desulfurization efficiency, rather than resolve the problems of dust-adhibiting, wall built-up and scaling in the production process. The existing researches that conducted numerical simulation of the gas-liquid flow field inside the desulfurization tower did not involve the process of acid-base absorption reaction, and thus failed to predict the amount of the reaction products and the their distribution in the desulfurization tower.

In order to solve the problems of dust-adhibiting and scaling during the production process in the rotary spray desulfurization tower, this paper establishes a mathematical-physical model to characterize the gas-liquid two-phase flow and the heat transfer and evaporation of droplets and a simulation model of the desulfurization reaction and the flow field calculation coupling in accordance with the absorption reaction mechanism of SO_2. To optimize the structure and operation parameters of the desulfurization tower, we take the on-site data as the boundary condition to study the influence of atomized particle with different diameters on the desulfurization efficiency and the amount of scaling on the inner wall of the tower. By setting baffles of various widths, the distribution of the flue gas in the upper and lower flue baffle and the flow field distribution of the flue gas in the desulfurization tower are optimized. By successfully resolving the problems of scaling and dust-adhibiting, the production can be carried out more smoothly and stably.

METHODS AND MODELS

Geometric model and grid generation

The external desulfurization tower consists of a cylinder part and a cone part, with the main components such as the inlet and outlet, flue, flue baffle, flue gas distributor, atomizing wheel and upper flue blade grid. The diameter of the desulfurization tower is 20.3 m, and the height is 40 m in total (see Fig. 2a). The height of the inlet flue is 8.9 m and its width reaches 6.8 m. With the weir-type flue gas distributor being installed at the lower inlet of the flue gas (see Fig. 2b), the flue gas goes through the upper or lower path after entering the desulfurization tower. Consisting of 120 blades, the blade grid is installed at the upper inlet of the flue gas with the inclined angle of each blade is 135°, which helps to change the flow direction of the flue gas. The length and width of the flue outlet are both 6 m. The alkali liquor is ejected through injection ports on the atomizing wheel. The diameter of the atomizing wheel is 360 mm and the injection port is 1 mm. Each atomizing wheel contains 12 injection ports.

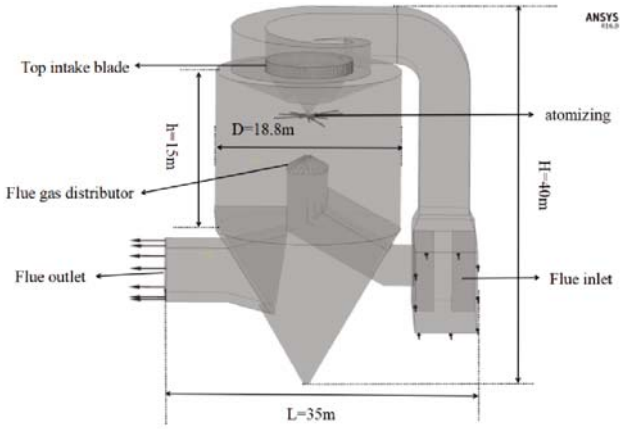

a. Geometry model of the SDA desulfurization tower

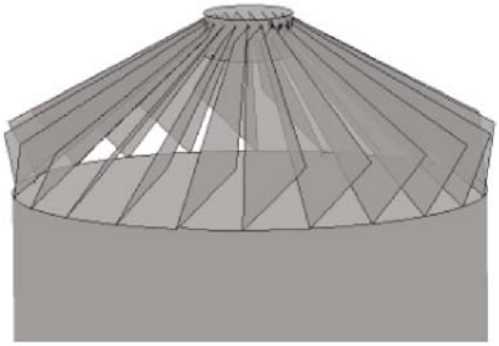

b. Geometry model of the weir-type flue gas distributor

Figure 2. The proposed model of the SDA desulfurization tower and the weir-type flue gas distributor

The tetrahedral unstructured grids are adopted to build the desulfurization tower (see Fig. 3). The girds are refined at the injection pores, the flue gas distributors and the blade grids to improve the calculation accuracy. This model includes 8,759,060 grid cells and 1,463,562 nodes in total.

Mathematical-physical model and chemical reaction

The flue gas inside the desulfurization tower is in form of incompressible turbulent flow. The alkali liquor is atomized into droplets with diameters ranging from 50 to 80 microns, and then ejected into the desulfurization tower. heated by the flue gas, the droplets will evaporate inside the tower, and then react with SO_2 in the flue gas. Therefore, this gas-liquid two-phase flow process involves the phase change and heat transfer.

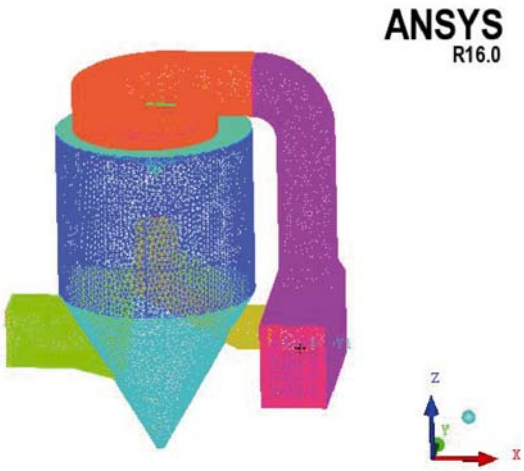

Figure 3. Grids of SDA desulfurization tower

Equation of flow control

(1) Continuity equation[28]

$$\frac{\partial \rho u}{\partial x}+\frac{\partial \rho v}{\partial y}+\frac{\partial \rho w}{\partial z}=0 \tag{1}$$

In the Equation (1), ρ refers to the fluid density, and u, v and w are the components of the velocity vectors at the directions of x, y and z, respectively.

(2) Momentum conservation equation[28]

$$\frac{\partial(\rho uu)}{\partial x}+\frac{\partial(\rho uv)}{\partial y}+\frac{\partial(\rho uw)}{\partial z}=\frac{\partial}{\partial x}\left((\mu+\mu_t)\frac{\partial u}{\partial x}\right)+\frac{\partial}{\partial y}\left((\mu+\mu_t)\frac{\partial u}{\partial y}\right)+\frac{\partial}{\partial z}\left((\mu+\mu_t)\frac{\partial u}{\partial z}\right)$$
$$-\frac{\partial p}{\partial x}+\frac{\partial}{\partial x}\left((\mu+\mu_t)\frac{\partial u}{\partial x}\right)+\frac{\partial}{\partial y}\left((\mu+\mu_t)\frac{\partial v}{\partial x}\right)+\frac{\partial}{\partial z}\left((\mu+\mu_t)\frac{\partial w}{\partial x}\right) \tag{2a}$$

$$\frac{\partial(\rho vu)}{\partial x}+\frac{\partial(\rho vv)}{\partial y}+\frac{\partial(\rho vw)}{\partial z}=\frac{\partial}{\partial x}\left((\mu+\mu_t)\frac{\partial v}{\partial x}\right)+\frac{\partial}{\partial y}\left((\mu+\mu_t)\frac{\partial v}{\partial y}\right)+\frac{\partial}{\partial z}\left((\mu+\mu_t)\frac{\partial v}{\partial z}\right)$$
$$-\frac{\partial p}{\partial y}+\frac{\partial}{\partial x}\left((\mu+\mu_t)\frac{\partial u}{\partial y}\right)+\frac{\partial}{\partial y}\left((\mu+\mu_t)\frac{\partial v}{\partial y}\right)+\frac{\partial}{\partial z}\left((\mu+\mu_t)\frac{\partial w}{\partial y}\right)-\rho g \tag{2b}$$

$$\frac{\partial(\rho wu)}{\partial x}+\frac{\partial(\rho wv)}{\partial y}+\frac{\partial(\rho ww)}{\partial z}=\frac{\partial}{\partial x}\left((\mu+\mu_t)\frac{\partial w}{\partial x}\right)+\frac{\partial}{\partial y}\left((\mu+\mu_t)\frac{\partial w}{\partial y}\right)+\frac{\partial}{\partial z}\left((\mu+\mu_t)\frac{\partial w}{\partial z}\right)$$
$$-\frac{\partial p}{\partial z}+\frac{\partial}{\partial x}\left((\mu+\mu_t)\frac{\partial u}{\partial z}\right)+\frac{\partial}{\partial y}\left((\mu+\mu_t)\frac{\partial v}{\partial z}\right)+\frac{\partial}{\partial z}\left((\mu+\mu_t)\frac{\partial w}{\partial z}\right) \tag{2c}$$

(3) Energy conservation equation[28]

$$\frac{\partial(\rho uT)}{\partial x}+\frac{\partial(\rho vT)}{\partial y}+\frac{\partial(\rho wT)}{\partial z}=\frac{\partial}{\partial x}\left(\frac{k}{c_p}\frac{\partial T}{\partial x}\right)+\frac{\partial}{\partial y}\left(\frac{k}{c_p}\frac{\partial T}{\partial y}\right)+\frac{\partial}{\partial z}\left(\frac{k}{c_p}\frac{\partial T}{\partial z}\right) \tag{3}$$

In the Equation (3), k represents the fluid heat transfer coefficient, which equals to 0.0332 W/m^2 · K. T is the fluid temperature, which is 403 K. cp is the specific heat at constant pressure, which is1004.4 J/kg K. ρ refers to the density, which is 0.8752 kg/m^3. μ is the turbulent viscosity, which is 2.32448 × 10^{-05} m^2/s.

(4) RNG $k-\varepsilon$ turbulence model[29]

The equation of the kinetic energy k and turbulent energy dissipation rate ε can be defined as follows:

$$\frac{\partial(\rho k u_i)}{\partial x_i}=\frac{\partial}{\partial x_j}\left(\alpha_k \mu_{eff}\frac{\partial k}{\partial x_j}\right)+G_k+\rho\varepsilon \tag{4}$$

$$\frac{\partial(\rho\varepsilon u_i)}{\partial x_i}=\frac{\partial}{\partial x_j}\left(\alpha_\varepsilon \mu_{eff}\frac{\partial \varepsilon}{\partial x_j}\right)+\frac{C_{1\varepsilon}^*\varepsilon}{k}G_k-C_{2\varepsilon}\rho\frac{\varepsilon^2}{k} \tag{5}$$

In the Equation (4) and (5), the turbulent viscosity coefficient $\mu_{eff}=\mu+\mu_t$. G_k is aterm of the turbulent kinetic energy k generated by the average velocity gradient, and its calculation formula is as follows:

$$\mu_t=\rho C_\mu\frac{k^2}{\varepsilon} \tag{6}$$

$$G_k=\mu_t\left(\frac{\partial u_i}{\partial x_j}+\frac{\partial u_j}{\partial x_i}\right)\frac{\partial u_i}{\partial x_j} \tag{7}$$

$$C_{1\varepsilon}^*=C_{1\varepsilon}-\frac{\eta(1-\eta/\eta_0)}{1+\beta\eta^3} \tag{8}$$

$$\eta=\left(2E_{ij}\cdot E_{ij}\right)^{1/2}\frac{k}{\varepsilon} \tag{9}$$

$$E_{ij}=\frac{1}{2}\left(\frac{\partial u_i}{\partial x_j}+\frac{\partial u_j}{\partial x_i}\right) \tag{10}$$

In the Equation (6) to (10), α_k and α_ε are the Prandtl numbers corresponding to the turbulent kinetic energy k and the dissipation rate ε, and their values are 1.39. β is the coefficient of thermal expansion, which is 0.012. $C_{1\varepsilon}$ and $C_{2\varepsilon}$ are the empirical constants, and their values are 1.42 and 1.68, respectively. The value of the constant η_0 is 4.377, while the value of the model constant C_μ is 0.0845[28].

Multiphase flow model

The Lagrange method was adopts to calculate the movement and evaporation of droplet particles. In the Lagrange coordinate system, the dispersed phase is analyzed in discrete particles, and the motion equation of each discrete particle is solved through integral. The movement trajectory of dispersed phase is obtained by taking the stress of the dispersed phase in the continuous phase and the turbulent diffusion trajectory into account. As for the continuous phase, the Navier-Stokes dynamic equation is solved in the Euler coordinate system. The motion equation of droplets is shown in the equation (11)[6]:

$$\frac{\partial u_p}{\partial t}=F_d(u-u_p)+\frac{g_x(\rho_p-\rho)}{\rho_p} \tag{11}$$

In this equation, $F_d(u-u_p)$ is the unit mass drag force of the particles, with the unit of N/kg. u represents the fluid velocity, with the unit of m/s. u_p represents the particle velocity. ρ_p is the particle density, and its unit is kg/m^3. The item $\frac{g_x(\rho_p-\rho)}{\rho_p}$ has taken the gravity and buoyancy of the particles into account.

When simulating two-phase flow, the particle coupling option was fully coupled. In the simulation, the drag force option was adopted as Schiller Naumann[32].

Chemical reaction of acid-base neutralization

The reaction between SO_2 and lime serous fluid is a continuous process, which contains the steps including the gas phase diffusion of SO_2, the absorption of SO_2 in water film, the ionization of SO_2 in water film, the transfer of acidic ions from aqueous layer to the reaction interface, the surface dissolution of absorbent, the transfer of the dissolved absorbent to the reaction interface, and finally the chemical reaction between the dissolved absorbent and the dissociated acid gas ions.

The alkali liquor contains water and calcium hydroxide. During the chemical reaction, Assuming that the calcium hydroxide molecules are thoroughly dissociated into ions, and the reaction is shown as follows:

$Ca(OH)_2 \rightarrow Ca^{2+} + 2OH^-$

SO_2 firstly reacts with the water in the serous fluid, forming the acid solution, which contains water and sulfuric acid. Assuming that the sulfuric acid molecules are completely dissociated into ions, the following reaction will occur:

$H_2SO_4 \rightarrow 2H^+ + SO_4^{2-}$

Moreover, Ca^{2+} will react with OH^-:

$Ca^{2+} + OH^- + SO_4^{2-} + H^+ \rightarrow CaSO_4 + H_2O$

In order to simulate the chemical reaction, it is assumed that the serous fluid is composed of single-molecule rigid droplet, the chemical reactions mainly takes place on the surface of the droplet instantaneously and irreversibly, and ignore the influence of the volume change under thermal evaporation on the chemical reactions.

Reactions and reaction kinetics can be modelled using CFX Expression Language (CEL), together with appropriate settings for Component sources. The reaction and reaction rate were modelled using a basic Eddy Break Up (EBU) formulation for the component and energy sources, so that, the transport equation for mass fraction of acid was

$$d\frac{\partial}{\partial t}(\rho mf_{acid}) + \nabla \cdot (\rho U mf_{acid}) - \nabla \cdot (\rho D_A \nabla mf_{acid}) = \\ = -4\rho \frac{\varepsilon}{k} \min\left(mf_{acid}, \frac{mf_{alkali}}{i}\right) \quad (12)$$

where *mf* is mass fraction, D_A is the Kinematic Diffusivity and *i* is the stoichiometric ratio. The right hand side represents the source term applied to the transport equation for the mass fraction of acid. The left hand side consists of the transient, advection and diffusion terms.

For acid-alkali reactions, the stoichiometric ratio is usually based on volume fractions. The reaction is modelled by introducing source terms for the acid, alkali and product components.

Simulation conditions

Material parameters

The main components of the flue gas are air and SO_2. The serous fluid consists of 20% of $Ca(OH)_2$ and 80% of water, with the mixed density of 1250 kg/m^3. The flue gas is regarded as the incompressible fluid. The impact of other components in the flue gas on the reaction is ignored.

Inlet conditions

The flue gas temperature reaches 130°C, and the inlet velocity of the flue gas is 6.88 m/s.

Outlet conditions

The outlet pressure is -1000 pa measured when the desulfurization tower is the operating.

Wall conditions

The wall surface, tower surface and bottom surface are heat insulation and designed to use rough material, with the roughness of 0.046 (equal to the roughness of steel). If the droplets are in the liquid when contacting the wall, they will lose their velocity in horizontal and vertical directions. If the droplets are dried before contacting to the smooth wall, the original flow field will not be affected.

Droplet spray parameters

The rotation speed of the atomizing wheel is 10000 r/min, ejecting droplets of serous fluid with a diameter of 30 to 70 μm. The mass flow rate of all ejection ports and temperature are 1.2 kg/s and 40°C respectively. The injection amount of $Ca(OH)_2$ in this paper is calculated by the amount of SO_2 measured in the literature. When the SO_2 concentration at the system outlet has reached the design requirement, n(Ca)/n(S) is equal to 1.28. The process of rotary atomization of the serous fluid is simplified and regarded as the serous fluid particles entering the desulfurization tower in accordance with the tangential direction of the rotation of the atomization wheel. That is, a tangential velocity represents the rotation process.

Initial conditions

In the simulation, the inlet velocity is used as the initial value of the flow filed. The initial static pressure and temperature of the calculation domain are 10^6 Pa and 130°C respectively. The turbulence intensity is 5%.

Verification of the calculation simulation model

The applicability and feasibility of the numerical calculation model can be verified through the measured data. The above-mentioned calculation model of the flow, heat transfer and chemical reaction is applied to the technological parameters of SDA, which is used for the No. 4 sintering machine of Shagang Group provided by Environmental Engineering[30]. The SO_2 concentration is calculated at the outlet, and compared with the measured value, to determine the accuracy and availability of the calculation model. The comparison of calculated value and measured value are shown in Figure 4.

The main operating parameters of the desulfurization tower in Environmental Engineering[30] are as follows: the average treatment capacity of flue gas is 2.04 million m^3/h, and the concentration of flue gas ranges from 4000 to 5000 mg/m^3, with the average flue gas temperature of 130°C and the highest temperature of 180°C. The rota-

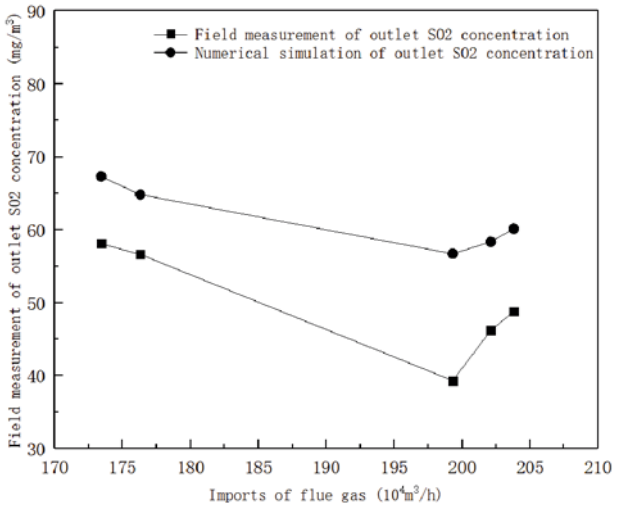

Figure 4. Comparison of experimental data and simulation data

tion speed of the serous fluid in the atomizing process is 10000 r/min, with the amount of spray serous fluid of 10.1876 to 24.3054 t/h. Meanwhile, the Ca/S ratio is 1.48 to 1.71m, which is higher than the theoretical design value of 1.2. The atomization diameter is 50 μm.

By comparison, it is found that the concentration of the flue gas at the outlet generated by numerical calculation is higher than the monitoring value, which means that the desulfurization efficiency is lower than the reality. The main reasons for this phenomenon are concluded as follows:

Firstly, the numerical study simplifies the components of flue gas at the inlet by neglecting the moisture and assumes the flue gas is composed of pure air and SO_2. However, there is 10% of water vapor in the sintering flue gas in the actual production. The water vapor impedes the evaporation of the serous fluid during the reaction, making the serous fluid left in liquid phase, but the desulfurization reacts mainly when the serous fluid are in liquid. Therefore, the reaction time of the serous fluid particles and the flue gas in the actual desulfurization process is longer than that of the numerical simulation, so that the actual concentration value of SO_2 in the flue gas after the desulfurization is lower than the calculated value.

Secondly, there is CO_2 in the flue gas in the actual reaction process, and $CaCO_3$ will be formed when CO_2 reacts with the serous fluid. Moreover, HSO_4^-, SO_3^{2-} and SO_4^{2-} ionized in the serous fluid will react with HCO_3^- and CO_3^{2-} in $CaCO_3$, according to the principle of replacing weak acid with strong acid. Therefore, the carbon dioxide will further improve the reaction efficiency, which makes the actual desulfurization efficiency higher than the calculated value.

The third reason is that as the utilization efficiency of the serous fluid is less than 100% in actual production, it is generally use excessive serous fluid to desulfurize the flue gas. According to the data provided by Gu, He and Jiang[30], the calcium-sulfur ratio ranges between 1.47 and 1.71 in actual operation. In calculation of this paper, the reaction coefficient is set as 1.2, which means that the ratio of the serous fluid and SO_2 is 1.2:1. To satisfy the requirement of actual production, the amount of spray serous fluid is relatively higher, so that the SO_2 are absorbed more thoroughly. Therefore, the calculated desulfurization efficiency is lower than actual value.

Numerical analysis

ANSYS ICEM[31] is employed to generate the 3D structural grids of the models. A high-resolution scheme is used to discretize the turbulence formulations. The high--resolution scheme uses the second order backward Euler scheme wherever and whenever possible and are reverted to the first order backward Euler scheme to maintain a bounded solution. The convection and diffusion terms of equations are discretized with the first-order upwind and central difference scheme, respectively. ANSYS CFX 16.0[32] commercial code is used to solve all governed equations. The under-relaxation factors for velocity, energy, and mass provided damping for the above equation set. In a steady-state calculation, the default value of 0.75 has been found to be sufficiently small to dampen solutions. The convergence criteria are that the values of root mean square of residuals are below 10^{-4}.

RESULTS AND DISCUSSION

The droplet diameter is a key factor which affects the evaporation and chemical reactions of the serous fluid. If the diameter of the droplet is too small, the droplet will rapidly evaporate once contacting to the flue gas, and the dry serous fluid particles will fail to react with SO_2, thus reducing the desulfurization efficiency. But if the diameter of the droplet is too large, the evaporation will be prolonged, and dust-adhibiting and scaling will be generated if the droplets are not dry enough when contacting to the inner wall of the desulfurization tower. Therefore, the movement trajectory of the droplets with different particle diameters under the same flue gas temperature and flue gas amount were studied.

The impact of droplet diameter on desulfurization efficiency

The droplets with the diameter of 30 μm, 40 μm, 50 μm, 60 μm and 70 μm are adopted for calculation. The movement trajectories of the droplets under different working conditions are shown in Fig. 5, and the evaporation time of the droplets are calculated by equation (13) and shown in Table 1.

$$\tau = \frac{L_w \rho_w}{(T_g - T_p)} \int_0^r \frac{1}{h} d_r \tag{13}$$

Where τis evaporation time, h refers to the heat transfer coefficient of the wet droplets and the air flow. T_g and T_p represent the temperature of the environment and the temperature of wet particles or droplets, respectively. L_w is the latent heat of water vaporization and d_r is droplet diameter.

Calculate the removal amount of SO_2 based on the concentration of SO_2 at the inlet and outlet, so as to explore the impact of the diameters of droplets on the desulfurization efficiency. The calculation formula of the desulfurization efficiency η is shown in the Equation (14):

$$\eta = \frac{c_{in} - c_{out}}{c_{in}} \tag{14}$$

In this equation, η represents the desulfurization efficiency. c_{in} is the concentration of SO_2 at the inlet, while c_{out} is the concentration of SO_2 at the outlet.

According to the comparative analysis in Figure 5a, the serous fluid will rapidly evaporate if the diameter of droplets is 30 μm, and the droplets will be dried within 0.55 s. According to the research results of Sang SK[33], if SO_2 fully contact with the wet surface of droplets, the change of the total surface area of droplets will become the key factor that impact the desulfurization. When the evaporation rate of droplets is too fast, the SO_2 fails to fully transfer to the surface of the droplets, so that the

Table 1. Evaporation time and desulfurization efficiency of droplets with different diameters

Diameter [μm]	30	40	50	60	70
Evaporation time [s]	0.55	0.72	0.9	1.1	1.26
Desulfurization efficiency [%]	81.3	87.5	95.5	97.0	97.5
Amount of scales [kg]	18.72	20.13	24.11	29.6	35.77

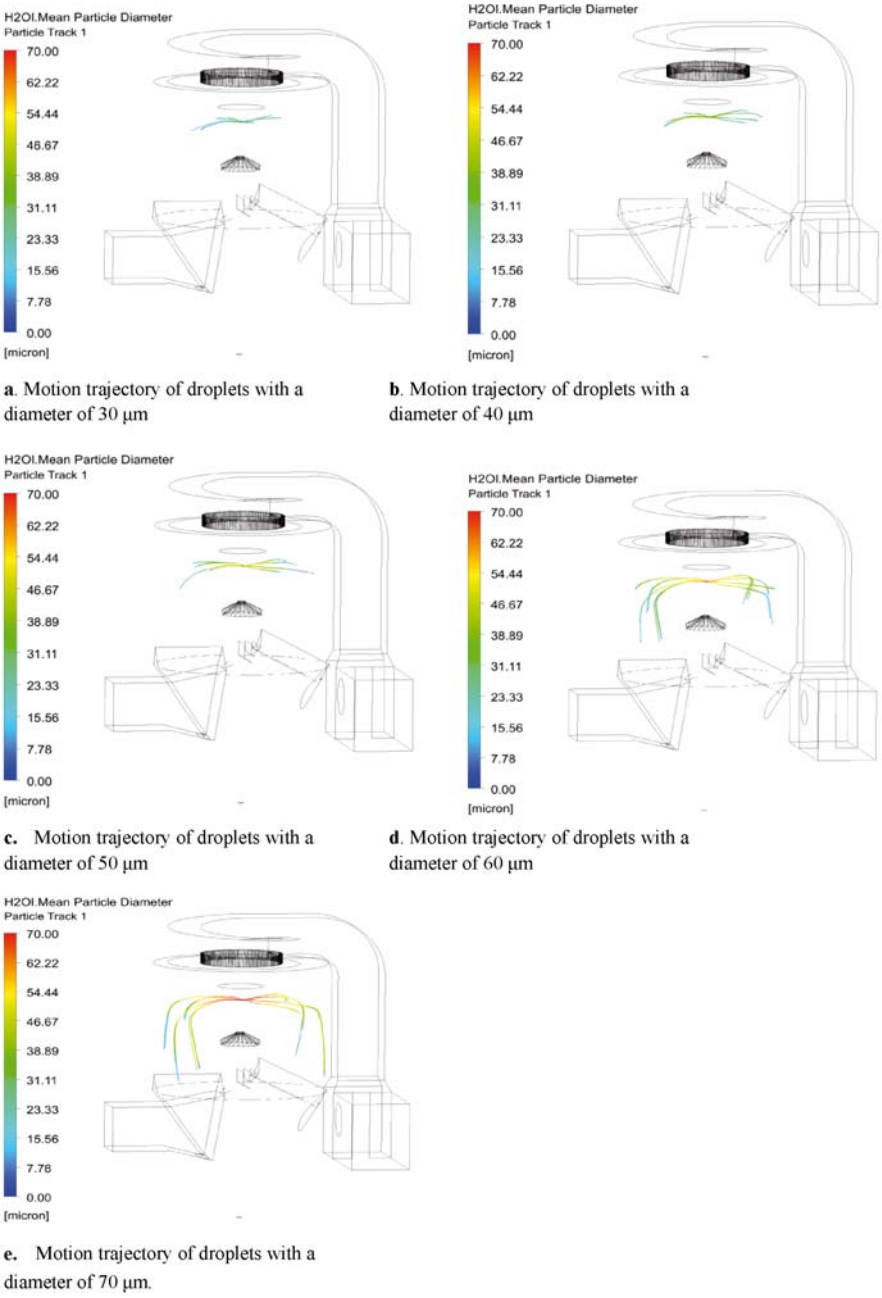

a. Motion trajectory of droplets with a diameter of 30 μm

b. Motion trajectory of droplets with a diameter of 40 μm

c. Motion trajectory of droplets with a diameter of 50 μm

d. Motion trajectory of droplets with a diameter of 60 μm

e. Motion trajectory of droplets with a diameter of 70 μm.

Figure 5. Motion trajectory of droplets with different diameters

serous fluid fails to react with SO_2 molecules effectively, thus reducing the desulfurization efficiency. Therefore, the desulfurization efficiency is relatively low when the diameter of droplets is 30 μm.

As shown in Figure 5b, when the diameter of particle of the serous fluid is 40 μm, the time required for the droplet evaporation reaches 0.72 s based on the calculation, which is longer compared with that of 30 μm. As a result, the desulfurization efficiency has been improved, but does not reach 95%, which fails to meet the requirement of production.

As shown in Figure 5c, when the diameter of droplet is 50 μm, the length of the movement trajectory is significantly increased. When contacting to the inner wall, the droplets are just in dry status, and the evaporation time of the serous fluid is about 0.9 s by calculation. The desulfurization efficiency is 95.5%, which fulfill the requirement of production. By observing the scaling amount, it can be found that as the diameter of the particles increases, the scaling amount increases significantly. Therefore, the particles with a diameter of 50 μm generate the minimal amount of scaling without reducing the desulfurization efficiency.

According to Figures 5e, when the droplet diameter is 70 μm, the evaporation of the serous fluid will be prolonged to 2.19 times than that of. droplet diameter 30 μm. In this case, more evaporation time means that serous fluid is given more time to absorb SO_2. Therefore, the desulfurization efficiency under this circumstance is higher than that of the droplet with other small diameters. However, it was also shown that since the serous fluid in liquid phase has not evaporated completely when contacting to the inner wall, the serous fluid would stick to the wall and produce scaling, which poses a negative impact on production. Thus, the particles with a diameter between 60 to70 μm are unsuitable for production, as the desulfurization efficiency fails to be significantly improved. Instead, the amount of scaling increases markedly

By analyzing Figure 5 and Table 1, it can be seen that the diameter of the serous fluid droplets has a great impact on the desulfurization efficiency. When the diameter of droplets

increases from 30 μm to 50 μm, the desulfurization efficiency increases 19.9%. When the diameter of droplet increases from 50 μm to 70 μm, the desulfurization efficiency just increases 2.1%, instead, the amount of scaling increases significantly. According to the national standard of China, the emission concentration of flue gas should be lower than 100 mg/m^3, while in this paper, the initial concentration of flue gas is 2000 mg/m^3. Therefore, the desulfurization efficiency should be higher than 95% to meet the requirements of sintering exhaust gas emission. In other word, the diameter of the droplets should be larger than 50 μm to meet the requirements of environmental protection for desulfurization. However, if the diameter of droplet is over 60 μm, there would generate 1.23 times scaling more than that case of 50 μm droplet, however the desulfurization efficiency only enhances 1.6%. The redundant scaling would blocks the paths in the desulfurization tower, and poses a threat to the stable production. Therefore, according to the simulation results, the droplets with a diameter of 50 μm is an optimum option which can ensure not only the high desulfurization efficiency, but also the stable operation of the desulfurization.

The impact of baffles of different widths on the amount of scaling inside the tower

The degree of completion of the desulfurization reaction is determined by the distribution of the flue gas inside the tower. When a large amount of flue gas flows through the spray area of the serous fluid evenly, the chemical reactants can fully contact and react with each other and SO_2 in the flue gas can be absorb to the maximum extent. If the flue gas is distributed unevenly and some of them fail to pass through the reaction zone, the short-circuited airflow will be formed. If the flue gas flows through the reaction zone too fast, SO_2 will not be absorbed completely, thus reducing the desulfurization efficiency. Moreover, excess serous fluid impacting the inner wall of the desulfurization tower will produce scaling through the chemical reaction, which adheres to the inner wall of the tower. The scaling is forms in two ways. Some are formed by unreacted and dry $Ca(OH)_2$ sticking to the inner wall after heated by the flue gas, and the others are salts generated by chemical reaction occurring close to the inner wall also under the influence of water mist.

In order to distribute the flow field evenly and promote reaction of the chemical reactants sufficiently, and reduce the scaling on the inner wall, it is proposed to fix a baffle at the inlet of the desulfurization tower (as shown in Fig. 6a). By adjusting the width of the baffle, the distribution ratio of the flue gas at the upper and lower sides of the inlet can be optimized. There are five types of baffles with the width ranging from 0 to 2.65 m in this study.

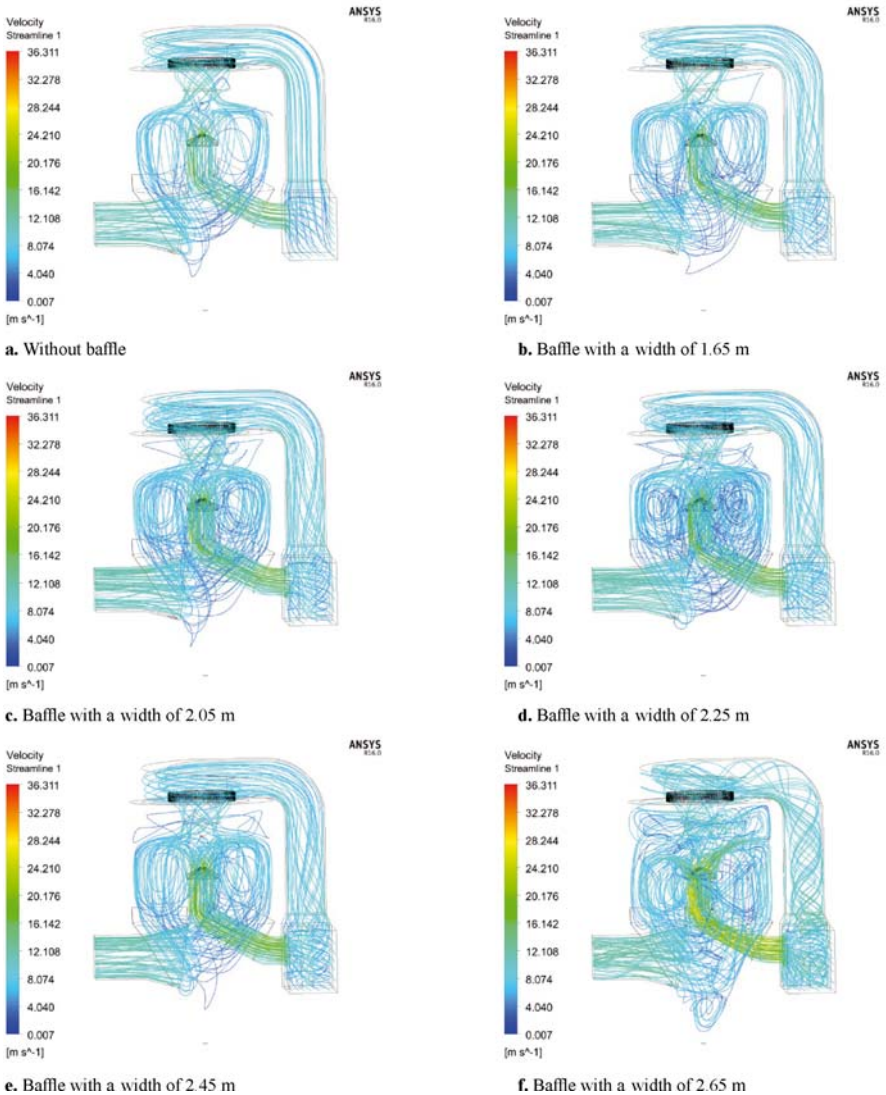

a. Without baffle **b.** Baffle with a width of 1.65 m

c. Baffle with a width of 2.05 m **d.** Baffle with a width of 2.25 m

e. Baffle with a width of 2.45 m **f.** Baffle with a width of 2.65 m

Figure 6. Flue gas streamline in tower with baffle of different width

As shown in Figure 6, the flue gas is divided into upper and lower two streams after entering the desulfurization tower. Entering the desulfurization tower through the rotary flue, the upper stream forms a vortex under the influence of the rotating inertia, and contacts and reacts with the alkaline droplets. Impacting the rotary atomizer, the lower stream also contacts with droplets in the middle of the desulfurization tower. Therefore, the flow ratio of the upper and lower stream has been regulated by the width of the baffle. By analyzing the Figure 6, it can be found that when the width of the baffle is 2.25 m, the stream lines reflect the flow trajectory of the flue gas concentrating inside the tower ,thus the flow field is quite disorder in the middle of the tower. It is also shown that there are less flow trajectory lines near the wall compared with other parts. Therefore, it can be predicted that amount of scaling on the wall will be the least under this circumstance.

As shown in Table 2, with the increase of width of baffle, the amount of the flue gas passing through the upper flue decreases, while the amount of the flue gas going through the lower flue increases. When the width of baffle increases from 0 to 2.25 m, the desulfurization efficiency increases 5%, but when the width of baffle increases from 2.25 to 2.65 m, the desulfurization efficiency decreases 3.25%. Therefore, at the point of acquiring the maximum desulfurization efficiency, the width of baffle should be 2.25 m.

On the other hand, the amount of scaling on the tower wall under the different baffle widths should be calculated and compared. The distribution and mass fraction of the resultants on the inside wall of the tower has been shown in Fig. 7.

Table 2. The flue gas distribution ratio, desulfurization efficiency and the amount of scaling with baffles of different widths

Width of the baffle [m]	0	1.65	2.05	2.25	2.45	2.65
The flue gas ratio at the upper and lower flues	0.82	0.75	0.69	0.67	0.61	0.6
Desulfurization efficiency [%]	91.71	93.43	96.22	96.79	94.62	93.64
Amount of scaling [kg]	36.0703	31.8014	29.1568	28.5883	29.7477	30.785

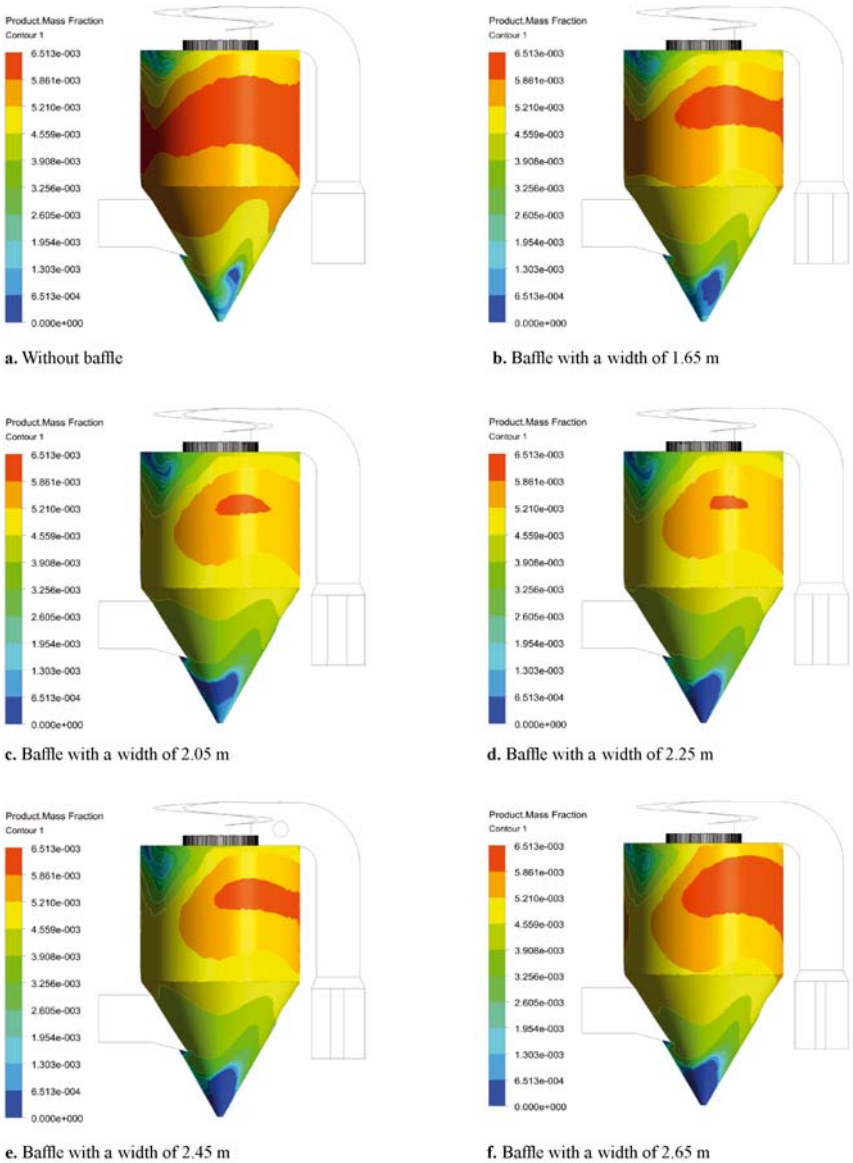

a. Without baffle **b.** Baffle with a width of 1.65 m

c. Baffle with a width of 2.05 m **d.** Baffle with a width of 2.25 m

e. Baffle with a width of 2.45 m **f.** Baffle with a width of 2.65 m

Figure 7. Distribution of scaling formed in the inner wall of tower with baffles of different width

It can be seen from Figure 7 that without any baffle, totally 36.07 kg scaling sticks to the inner wall of the tower, which blocks the flow channel. As a result, the production must be stopped frequently to clean the tower. With the width of the baffle increasing to 2.25 m, the flue gas ratio of upper and lower stream is 0.67, and the amount of scaling is 28.5883 kg which is the least among all study cases. However, when the width of the baffle is larger than 2.25 m, the balance of flow field is broken, redundant flue gas from lower smoke pipe is unevaporated and contacts to the inner wall, so 2 kg more scaling generates, which impedes the production. Therefore, the baffle with a width of 2.25 m is the optimal option for production, with a higher desulfurization efficiency and the least scaling on the inner wall of the desulfurization tower.

CONCLUSION

This paper studies the flow field and desulfurization efficiency in the rotary spray tower using the method of numerical simulation with the coupling of chemical reactions. By comparing the calculated concentration of SO_2 at the outlet with the monitoring values, this paper verifies the correctness of stimulating the gas-liquid two--phase flow field in the desulfurization tower through the RNG k–ε turbulence model and the particle trajectory physical model coupling chemical reaction.

It has been found that the diameter of the serous fluid droplets significantly impact the desulfurization efficiency. The desulfurization efficiency is improved with the increase of the droplet diameter. However, if the droplet diameter is too large, as the serous fluid is still wet when contacting to the tower wall, a large amount of scaling will be produced, which blocks the desulfurization tower and impedes the stable operation of production. The droplet with a diameter of 50 μm is an optimum parameter which can ensure not only the high desulfurization efficiency, but also the stable operation of the desulfurization.

The distribution of the flue gas inside the tower affects the completion level of the desulfurization reaction. Installing plate baffle can regulate the flow ratio of the upper to the lower stream. With the width of the baffle increasing, the upper stream decreases while the upper stream increases. When the width of baffle is 2.25 m, the desulfurization efficiency in the tower reaches the maximum, and the amount of the scaling on the surface of the tower wall is the least, which meets the requirements of production.

ACKNOWLEDGEMENT

This paper is supported by Hubei Province Natural Science Foundation of China (project number: 20171105) and Hubei Key Laboratory of Industrial Fume & Dust Pollution Control (project number: HBIK2016-04).

LITERATURE CITED

Feng, Yu-zhi. & Wang, Ying-gang. (2000). The harms and preservation of sulfur dioxide to industrial workers. On-Ferrous Mining and Metallurgy. 1, 47–48.

2. Rao, Zhi-jun. (2005). Research on rotary spray technology and its electromechanical system. Tianjin University. DOI: 10.7666/d.y848955.

3. Liu, Yong-feng, Wei, Chuan-wen & Zhang, Xu. (2008). Suitable sintered flue gas desulfurization for SDA technology. *China Steel. Pap*. (5), 32–33. DOI: 10.3969/j.issn.1672-5115.2008.05.009.

4. Lan, Guo-qian, Liu, Jian-qiu & Zhang, Jiang-wei. (2014). Present situation and trends of the sintering flue gas Desulphurization in iron and steel industry. *China Enwiron. Protec. Ind.* (6), 42–46. DOI: 10.3969/j.issn.1006-5377.2014.06.012.

5. Hans, T., Karlsson & Jonas, Klingspor. (1987). Tentative modelling of spray-dry scrubbing of SO_2. *Chem. Engin. Technol.* 10(1), 104–112. DOI: 10.1002/ceat.270100114.

6. Hill, F.F. & Zank, J. (2000). Flue gas desulphurization by spray dry absorption. *Chem. Eng. Proce.* 39(1), 45–52. DOI: 10.1016/S0255-2701(99)00077-X.

7. Gullett, B.K. (1987). Fundamental process involved in SO_2 capture by calcium-based adsorbents. Fourth Annual Pittsburgh coal conference. OSTI: 5790586.

8. Xu, G., Guo, Q., Kaneko, T. & et al. (2000). A new semi-dry desulfurization process using a powder-particle spouted bed. *Adv. Enwiron. Res.* 4(1), 9–18. DOI: 10.1016/S1093-0191(00)00003-4.

9. Dantuluri, S.R., Davis, W.T., Counce, R.M. & et al. (1990). Mathematical model of sulfur dioxide absorption into a calcium hydroxide slurry in a spray dryer. *Chem. Engin. Commun.* 25(13–15), 1843–1855. DOI: 10.1080/01496399008050428.

10. Wentz, T.H. & Thygeson, J.R. (1979). Handbook of separation technique for chemical engineers, chapter 4.10, MaGraw-Hill. DOI: 10.1002/aic.690260238.

11. Ranz, W.F. & Marshall, W.R. (1952). Evaporation from drops. *Chem. Engin.* 48(3), 141–146. DOI:

12. Partridge, G.P., Davis, W.T. & Robert, M. (1990). Counce and Gregory D. Reed. A mechanistically based mathematical model of sulfur dioxide absorption into a calcium hydroxide slurry in a spray dryer. *Chem. Engin. Commun.* 96(8), 97–112. DOI: 10.1080/00986449008911485.

13. And, H.M.Y. & Sang, S.K. (2000). Experimental study on the spray characteristics in the Spray Drying Absorber. *Environ. Sci. Technol.* 34(21), 4582–4586. DOI: 10.1021/es001104c.

14. Keener, T.C., Wang, J. & Khang, S.J. (1998). Advances in spray drying desulfurization for high-sulfur coals. Dry scrubbing technologies for flue gas desulfurization. Springer US. Pap. 607–690. DOI: 10.1007/978-1-4615-4951-2_8.

15. Cheng, Ming-gong & Zhi-You-gang. (2000). Theoretical analysis of desulfurization influence factors of flue gas. *Jiangsu Environ. Sci. Technol.* 13(1), 1–3. DOI: CNKI:SUN:J-SHJ.0.2000-01-000.

16. Kim, H. & Sung, N. (2003). The effect of ambient pressure on the evaporation of a single droplet and a spray. *Combus. Flame.* 135(3), 261–270. DOI: 10.1016/S0010-2180(03)00165-2.

17. Kang, Mei-qiang. (2013). Study on flue gas desulfurization wastewater duct evaporation treatment system design and experiment. Chongqing University. DOI: 10.7666/d.D354464.

18. Han, Fang-liang, Li, Guo-hua & Xu, Ning. (2006). Parameters simulation of flow field in spray drying flue gas desulfurization tower. *China Water Transport.* 6(10), 66–68. DOI: CNKI:SUN:SYZB.0.2006-10-029.

19. Scala, F., D'Ascenzo, M. & Lancia, A. (2004). Modeling flue gas desulfurization by spray-dry absorption. *Separ. Purfic. Technol.* 34(1), 143–153. DOI: 10.1016/S1383-5866(03)00188-6.

20. Karlsson, H.T. & Klingspor, J. (1987). Tentative modelling of spray-dry scrubbing of SO_2. *Chem. Eng. Technol.* 10(1), 104–112. DOI: 10.1002/ceat.270100114.

21. Scala, F. & D'Ascenzo, M. (2002). Absorption with instantaneous reaction in a droplet with sparingly soluble fines. *Aiche Journal*. 48(8), 1719–1726. DOI: 10.1002/aic.690480813.

22. Chen, Jian-zhong. (2017). Study on coke oven desulfurization and the reheat of sintering flue gas before denitrification. Zhejiang University.

23. Wang, Nai-hua. (2001). Experimental and mechanism analysis of a novel semi-dry flue gas desulfurization. Zhejiang University.

24. Qin, Lin-bo & Han, Jun. (2017). Simultaneous removal of SO_2 and PAHs by adding calcium-based additives during sewage sludge incineration in a fluidized bed incinerator. *J. Mater. Cycles Waste Manag.* 19(3), 1061–1068. DOI: 10.1007/s10163-017-0592-6.

25. Qin, Lin-bo & Han, Jun. (2016). Experimental study on SO_2 removal during novel integrated desulfurization process. *Fres. Environ. Bull.* 25(11), 4561–4565. DOI: 10.1142/9789813143401_0056.

26. Liu, Huan. (2016). Co-production of clean syngas and ash adsorbent during sewage sludge gasification: Synergistic effect of Fenton peroxidation and CaO conditioning. *Apll. Energy.* 179, 1062–1068. DOI: 10.1016/j.apenergy.2016.07.063

27. Qin, Lin-bo & Han, Jun. (2017). Enhancing SO_2 removal efficiency by lime modified with sewage sludge in a novel integrated desulfurization process. *Environ. Protec. Engin.* 43(4), 17–27. DOI:

28. Wang, Fu-jun. (2004). Computational fluid dynamics analysis: principles and applications of CFD software. Tsinghua University Press, Beijing.

29. Cheng, W.C., Liu, C.H. & Leung, D.Y.C. (2009). On the correlation if air and pollutant exchange for street canyons in combined wind-buoyancy-driven flow. *Atmosp. Environ.* 43(24), 3682–3690. DOI: 10.1016/j.atmosenv.2009.04.054.

30. Gu Bing, He Shen-fu & Jiang Chuang-ye. (2013). Application of spray drying absorption (SDA) in desulphurization of sintering flue gas. *Environ. Engin.* 31(2), 53–56. DOI: 10.13205/j.hjgc.201302015.

31. ANSYS ICEM CFD user guide. (2016). Ansys Inc.

32. ANSYS CFX user guide. (2016). Ansys Inc.

33. Dantuluri, S.R., Davis, W.T., Counce, R.M. & et al. (1990). Mathematical model of sulfur dioxide absorption into a calcium hydroxide slurry in a spray dryer. *Chem. Engin. Commun.* 25(13–15), 1843–1855. DOI: 10.1080/01496399008050428.